J Mater Sci (2008) 43:7280–7285
DOI 10.1007/s10853-008-2673-3

ULTRAFINE-GRAINED MATERIALS

The effect of cryogenic deformation on the limiting grain size in an SMG Al-alloy

P. B. Prangnell · Y. Huang

Received: 31 January 2008 / Accepted: 22 April 2008 / Published online: 13 July 2008

Abstract The minimum grain size obtainable in an Al–0.1%Mg submicron grained (SMG) alloy, subjected to cryogenic plane strain deformation, and its subsequent stability during room temperature deformation have been investigated. A decreasing steady state grain size was obtained with reducing deformation temperature. However, a true nanocrystalline grain structure was not obtained even at 77 K with the high angle boundary spacing only approaching the nanoscale in the sample normal direction. The cryogenically deformed material was unstable on subsequent deformation at room temperature and underwent rapid dynamic grain growth. Dynamic grain coarsening is shown to limit the minimum grain size achievable in an SPD process, even under cryogenic conditions.

Introduction

At the ultra-high strains seen in severe plastic deformation (SPD) a steady state grain size is ultimately approached which restricts the level of grain refinement that can be achieved [1–3]. For example, during equal channel angular extrusion (ECAE) of Al-alloys, the high angle boundary (HAB) spacing reaches a minimum when it converges with subgrain size and the fraction of HAB area typically saturates at ~70–80% [1]. This limiting grain size has been attributed to dynamic recovery [1, 2, 4]. However, the restoration processes involved are still poorly understood [4].

P. B. Prangnell (✉) · Y. Huang
Manchester Materials Science Centre, The University of Manchester, Grosvenor Street, Manchester M17HS, UK
e-mail: philip.prangnell@manchester.ac.uk

Y. Huang
e-mail: Yan.huang-2@manchester.ac.uk

Similar to steady state subgrain sizes [5], the minimum grain size achievable in an SPD process is thought to be related to the temperature compensated strain rate, or Zener-Holloman parameter (Z) [2, 4]. It is, therefore, possible to achieve a smaller grain size by lowering the deformation temperature, which results in the suppression of thermally activated recovery processes. Indeed, cryogenic deformation has been claimed to lead to the formation of nanocrystalline structures in Cu and other alloys [6–8] offering the prospect of being able to produce nanograined materials by SPD in a bulk form. Typically, this involves heavily rolling materials at liquid nitrogen temperatures, which have already been deformed by a SPD technique like ECAE to develop a starting submicron grain structure [6, 7].

Because of the fine nanoscale of the crystallite sizes produced in cryogenic SPD processing, much of the information in the literature is based on TEM evidence (e.g. [6–8]). As a result, reliable data has frequently not been obtained that fully characterizes the misorientations of the boundaries within the materials. It is thus often unclear whether the deformation structures produced are true nanograin structures or still contain a large fraction of low angle boundaries (LABs). In addition, nanograined materials produced by deformation at cryogenic temperatures are likely to be unstable at room temperature, due to their highly non-equilibrium internal state. A potential concern is the rapid dynamic grain coarsening that has been reported to occur during deformation of nanograined materials manufactured by vapour deposition routes [9–12]. This phenomenon has not been extensively investigated in severely deformed alloys, but is related to the same restoration processes that control the limiting grain size during SPD processing.

The aim of the work presented is to investigate the effect of low temperatures on the minimum grain size that can be

obtained by SPD processing of Al-alloys, with the goal of producing a true nanograined material (i.e. with a HAB spacing of <100 nm in all dimensions). The stability of the structures produced under dynamic conditions was also of interest. This was achieved by studying a dilute Al-alloy, deformed cryogenically by plane strain compression, following pre-processing by ECAE to give a starting submicron grain structure. The results are, therefore, inline with the processing route adopted by several other studies in the literature (e.g. [6, 7]).

Experimental

A single phase Al–0.13 wt% Mg alloy was cast, cold rolled 50%, and recrystallized to give an initial grain size of ~300 μm. Billets 100 mm long by 15 mm square cross-section billets were machined in the rolling direction and pre-processed by 15 ECAE passes via route A, through a 120° die at 298 K, to a total effective strain of ~10 ($\varepsilon \sim 0.3\ s^{-1}$). Plane strain compression (PSC) specimens 12 × 8×10 mm were subsequently cut from the ECAE billets and deformed in a channel die to a true strain of $\varepsilon_{tr} = 2.8$, ($\varepsilon \sim 10^{-2}\ s^{-1}$). Channel die PSC was chosen to simulate rolling under more controllable conditions of constant temperature and strain rate. During deformation the PSC rig and samples were immersed in baths, chilled with liquid nitrogen, to obtain temperatures from 298 K down to 77 K ± 2 K. Following PSC at 77 K, some samples were rolled at room temperature to an additional true strain of 2.8.

The deformed samples were sectioned through their centre in the ND-RD plane and characterized by high resolution electron back scatter diffraction (EBSD) orientation mapping in an FEI Siron(TM) field emission gun scanning electron microscope (FEGSEM) with an HKL technology(TM) EBSD system. In a channel die, ND is equivalent to the normal direction in rolling and parallel to the direction of sample compression, whereas RD is the direction of sample extension and equivalent to the rolling direction. The spatial and angular resolutions of the EBSD system were ~10 nm and ~1°. In the maps HABs are shown by black lines and have misorientations ≥15°, while LABs are depicted by white lines and have misorientations <15°. Due to misorientation noise, boundaries were cut-off of at less than 1.5°. Average linear intercept measurements of the HAB and LAB spacings were made in ND (defined as λ_{ND}) and rolling or extrusion direction (described as λ_{RD}), as well as the fraction of HAB area and average boundary misorientations. For each measurement, data from several maps were used to obtain averages over ~2,000 grains. λ_{RD} was measured by manual line scanning, as small deviations from alignment with the reference frame by thin ribbon grains led to unrealistically low aspect ratios with the EBSD analysis software.

Results and discussion

Cryogenic PSC processing

Examples of deformation structures seen in the ECAE pre-processed submicron grained SMG material and during cryogenic PSC at different temperatures and strains are shown in Fig. 1. Statistical data from the EBSD maps is given in Fig. 2. The deformation structures formed by ECAE processing at room temperature and the grain refinement mechanisms involved have been previously reported (e.g. [1, 13]). At a strain of ten, processing by route A leads to the development of a fibrous deformation structure comprising a mixture of elongated thin ribbon grains and lower aspect ratio submicron grains, with a significant proportion of retained transverse LABs. The ECAE processed starting material had a transverse HAB spacing, or grain width, of $\lambda_{ND} \sim 0.55$ μm, grain aspect ratio of ~2.3, and fraction of HAB area ~75%. Previous work has shown that the grain width, λ_{ND}, continues to decrease only extremely slowly at higher strains in ECAE and can be considered to have already approached a pseudo-steady state by a strain of ten [1, 13].

For channel die plane strain compression the grain structure inherited from pre-ECAE processing was aligned, such that the direction of grain elongation was approximately parallel to RD and the compression direction parallel to the grain width, ND. If a material deforms homogeneously in PSC, this will result in a tendency to reduce the grain width in ND and extend grain boundaries parallel to RD. If on average the grain shape is directly coupled to the strain tensor, in PSC the transverse HAB spacing is geometrically required to reduce in proportion to the sample reduction ratio and can be related to the initial grain width, λ_0, and true strain, ε_{true}, [4] by;

$$\lambda_G = \lambda_0 \exp(-\varepsilon_{true}) \quad (1)$$

The theoretically predicted geometric reduction in HAB spacing, λ_G, is plotted along with the measured values of HAB spacing, λ_{ND}, in Fig. 2a. In room temperature PSC, only a small reduction in grain size was observed (Fig. 2a). The theoretical curve, λ_G, can be seen to decrease more rapidly than the measured spacing and continue to fall with increasing strain, while the measured rate of reduction in λ_{ND} quickly falls off and approaches a new pseudo-steady grain width. This results in only a small reduction in λ_{ND} from 0.55 to 0.42 μm. Without a simultaneous increase in Z, the change in deformation mode from ECAE to PSC, therefore, merely gives rise to a small readjustment of the

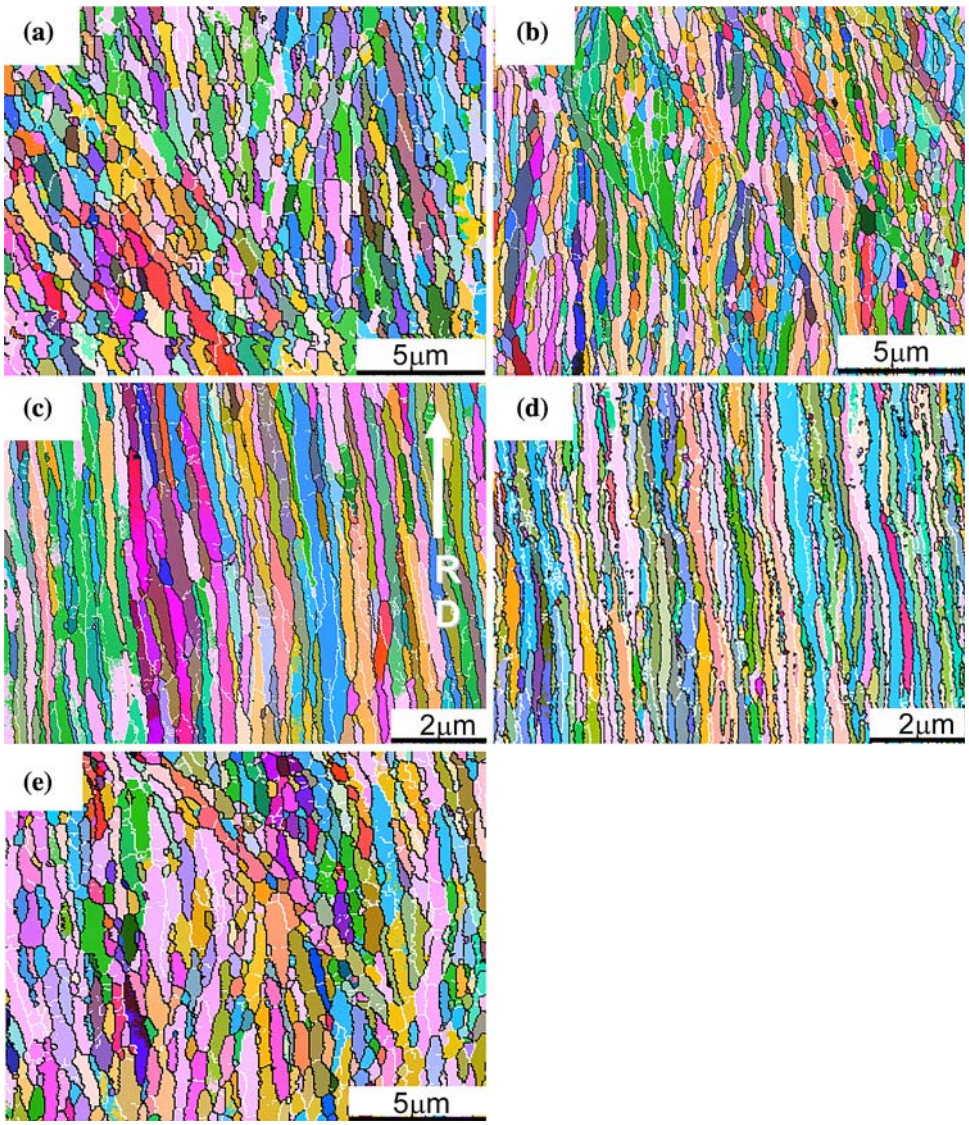

Fig. 1 EBSD orientation maps showing example deformation structures from cryogenic PSC samples deformed; (**a**) at 298 K, (**b**) 213 K, (**c**) 77 K, to a strain of $\varepsilon_{tr} = 2.1$, and (**d**) to a strain of $\varepsilon_{tr} = 2.8$ at 77 K. In (**e**) the deformation structure is shown of a sample first deformed by PSC at 77 K following rolling at 298 K to a further strain of $\varepsilon_{tr} = 2.8$. Note the different scales

deformation structure and the rapid attainment of a new minimum HAB spacing.

As the deformation temperature is lowered, in Fig. 2a, the transverse boundary spacing, λ_{ND}, initially closely follows the predictions of Eq. 1 to larger strains with reducing temperature, before again rapidly slowing down and approaching a pseudo-steady state at higher strains. Departure from the theoretical λ_G curve occurs more slowly the colder the deformation temperature, and the strain required to approach a constant λ_{ND} increases, from $\sim$0.6 at room temperature to $\sim$1.2 at 77 K, resulting in a larger reduction in grain width with decreasing temperature. A similar behaviour was observed for the grain aspect ratio, which also initially closely followed the curve predicted from λ_G at low strains and increased dramatically with reducing deformation temperature, from $\sim$2.3 to 15 at 77 K. With decreasing temperature (Fig. 1a–c), the starting UFG structure thus becomes highly elongated parallel to RD and at 77 K a very fine lamellar grain structure was formed. Figure 1d shows the extremely elongated ribbon grain microstructure obtained at 77 K, with the maximum strain that could be achieved of $\varepsilon_{true} = 2.8$. The average transverse boundary spacing (including both LABs and HABs) in the PSC samples was 130 nm, which is verging on being nanocrystalline. However, if only boundaries greater than 15° in misorientation are considered, the minimum HAB spacing achieved in ND was 180 nm. In comparison, the average HAB spacing in RD at this temperature was estimated to be $\sim$3.0 μm, which is greater than that seen in the ECAE processed starting material, with some ribbon grains extending for up to ten microns long.

From Fig. 2b it can be observed that on changing the deformation mode to PSC there is an initial decrease in HAB area fraction, which becomes more pronounced as the deformation temperature is reduced. This results from the

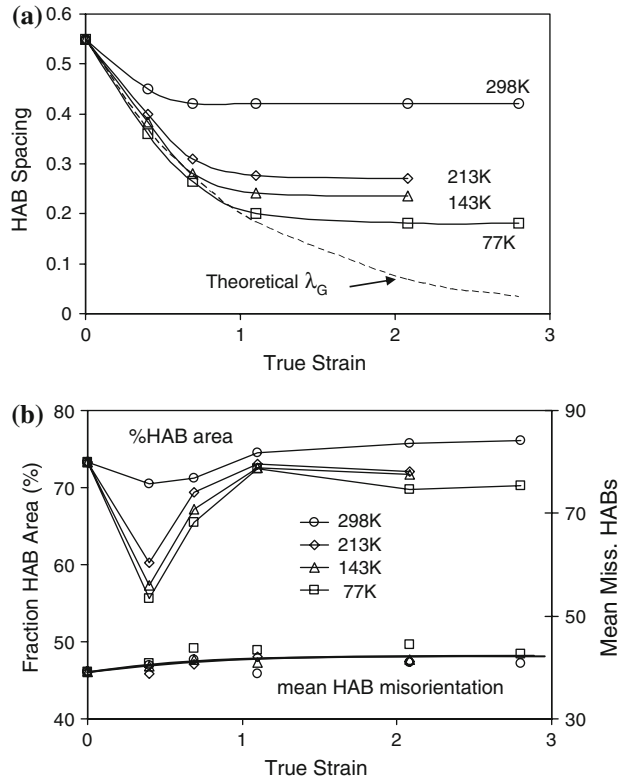

Fig. 2 Statistical data obtained from EBSD maps showing; (**a**) the transverse HAB spacing, λ_{ND}, and theoretically predicted grain width, λ_G, and (**b**) the fraction of HAB area and mean HAB misorientation, with strain, as a function of cryogenic temperature

introduction of new LABs at the onset of PSC, as the equilibrium cell size is decreased by the reduction in temperature. The HAB fraction then increases with further strain at all temperatures, approaching a similar level close to that of the starting material by a strain of $\varepsilon_{true} > 1.1$. In comparison, the average HAB misorientations all behaved similarly, irrespective of temperature, and appeared to increase marginally on plane strain compression to $\varepsilon_{true} = 2.8$. Little evidence of grain subdivision was found in the EBSD maps during deformation of any of the PSC samples. This, and the fact that at low temperatures λ_{ND} and the grain aspect ratio initially closely follow the theoretical predicted curves from equation 1, before departing to reach limiting values, suggests that the increase in HAB area that occurs on PSC of an SMG material is primarily due to the extension of pre-existing boundaries and the compression of their spacing in proportion to the geometric shape change of the sample.

At temperatures down to 143 K the deformation structures in the PSC samples were disrupted by the appearance of shear bands (Fig. 1a, b). The shear bands reduced in width and intensity with decreasing temperature until they completely vanished at 77 K (Fig. 1d). Shear, or Lűders, bands have been widely reported during uniaxial testing of SMG alloys (e.g. [14]). During deformation of ultra-fine grained materials there is little dislocation storage within grains resulting in a near zero work hardening rate [14]. Changing the deformation mode from shear to PSC further results in the activation of latent slip systems and a realignment of the shear plane, relative to the orientation of the substructural boundaries. Both of these factors are known to promote shear instability [15]. At low temperatures the material will recover some strain hardening capacity, as is evident from the initial increase in LAB area seen in Fig. 2b, and it is thus not surprising that the intensity of shear banding reduced with temperature, disappearing completely at 77 K.

The effect of room temperature deformation on grain structure stability

From Fig. 3 it can be seen that samples stored up to 6 months at room temperature, with no further deformation, showed only a slight increase in spacing of their lamellar HABs, by $\sim$0.02 μm. In comparison, when specimens previously deformed by PSC at 77 K were subsequently rolled at room temperature, λ_{ND} rapidly increased from 0.18 to 0.43 μm and reached a stable value with a similar level to that seen in the samples directly compressed at room temperature. Furthermore, from comparing Fig. 1a and d, it can be seen that on reverting to rolling at room temperature after PSC at 77 K, the deformation structures became remarkably similar to those seen after continuous PSC at room temperature. This suggests that the HAB spacing re-adjusts towards a pseudo-steady

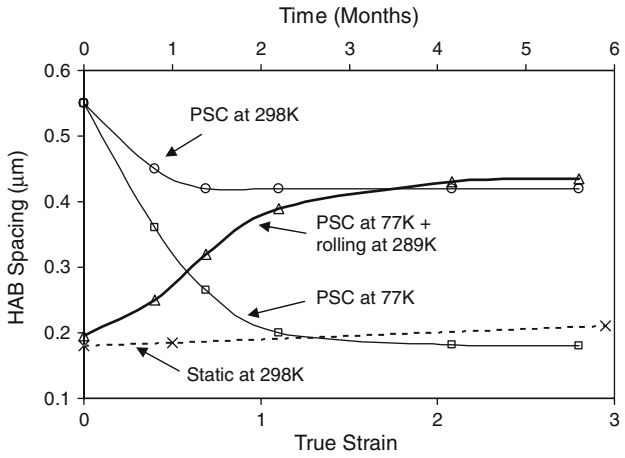

Fig. 3 λ_{ND} plotted against storage time and strain during deformation by rolling at room temperature, after channel die plane strain compression (PSC) at 77 K, compared to normal PSC deformation at 298 and 77 K

state grain size, in response to a change in Z, at a rate that is far higher than possible under static annealing conditions.

Dynamic grain coarsening in SPD

It is clear from the above evidence that a pseudo-steady state HAB boundary spacing is approached, irrespective of the deformation temperature, which controls the minimum grain size that can be achieved in an SPD process. Furthermore, on increasing the deformation temperature the HAB spacing readjusts to the same steady state spacing seen on uninterrupted deformation at the same temperature. This occurs at a far higher rate than is possible under static conditions. The minimum boundary spacing achievable is thus controlled by equilibrium being established between the rate of compression of the HAB spacing, in response to the strain, and dynamic boundary migration, or grain coarsening. It is of course possible that deformation is accommodated by an alternative mechanism, such as grain boundary sliding, but this seems unlikely given the low temperature and grain structure evolution observed, which resulted in a lamellar HAB structure.

To maintain a steady state transverse HAB spacing, $\lambda_{ND,}$ boundaries must migrate at a rate equal to that of their compression, V_C, which can be related to the strain rate, $\dot{\varepsilon}$, by:

$$V_C = \frac{d\lambda}{dt} = \dot{\varepsilon}\lambda_{ND} \tag{2}$$

The boundary migration rate is usually assumed to be proportional to the driving force, P, and mobility, M.

$$V_M = PM \tag{3}$$

Following the approach detailed by Humphreys [4], if it is assumed that the average driving force is related to HAB boundary curvature, then

$$P = \frac{\gamma}{4R} \tag{4}$$

where R is the radius of curvature and γ the HAB energy. If it is assumed that $\lambda_{ND} = 2R$ and taking $\gamma = 0.32$ J m^{-2}, then values of the estimated rate of boundary compression, taken from the EBSD maps using Eq. 2, can be normalized relative to the pressure and plotted against inverse temperature in Fig. 4. As diffusion controlled boundary mobility is given by:

$$M = M_o \exp\left[\frac{-Q}{RT}\right] \tag{5}$$

the activation energy for diffusion controlled boundary migration can then be taken from the slope of the data in Fig. 4, where two regimes can be seen. Above room temperature the steeper slope implies an activation energy of $\sim$60 kJ mol^{-1}, as opposed to $\sim$130 kJ mol^{-1} for convectional diffusion controlled migration at elevated

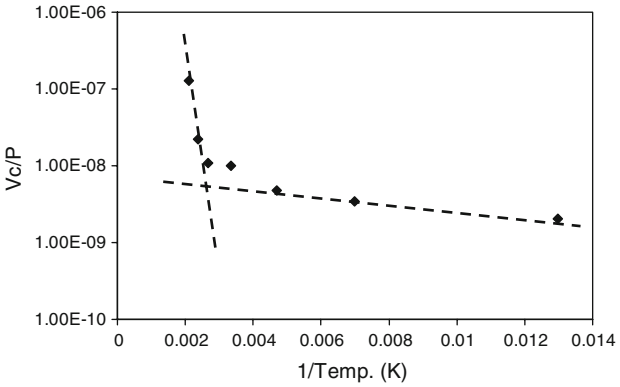

Fig. 4 HAB migration rates normalized with respect to surface tension driven pressure (V_C/P) required to maintain a constant spacing during geometric compression plotted against inverse temperature, including data from 100 to 200 °C for the same SMG starting material

temperatures [4], whereas below 298 K the much shallower slope suggests an apparent 'activation energy' as low as $\sim$1 kJ mol^{-1}, which is physically unreasonable for a diffusion controlled process. The activation energy from room temperature and above is inline with expected values for either grain boundary or vacancy diffusion in aluminium [16, 17], which would be typical of the behaviour of a disordered non-equilibrium boundary structure and/or due to the presence of a high non-equilibrium vacancy concentration, both of which might be expected under dynamic conditions [18, 19]. Below room temperature the migration rate is many orders of magnitude higher than can be explained by diffusion controlled growth.

This enhanced boundary migration rate is important because it controls the limiting grain size achievable by an SPD process, although it is difficult to explain. No reasonable increase in driving force, due to factors such as dislocation, storage or inter-granular stresses, can account for this discrepancy. Furthermore, alternative mechanisms, such as solute breakaway, have activation energies similar to that for grain boundary diffusion (60 kJ mol^{-1} in Al–Mg alloys [20]).

One possibility is that of stress induced boundary migration, which has been proposed when associated with solute breakaway, to explain the similarly abnormal rapid grain growth seen during tensile deformation of nanocrystalline thin films at cryogenic temperatures [10]. Molecular dynamics simulations and experimental measurements have shown that high angle boundaries can migrate under the action of an applied shear stress [17, 21]. At very low stresses Winning et al. [17] have found that for planar tilt boundaries the migration rate is proportional to the applied shear stress, but in this work boundary migration was found to be controlled by the climb of structural GB dislocation segments, and the activation energy was measured to be $\sim$0.8 eV (77 kJ mol^{-1}), which is again

close to the accepted value for grain boundary diffusion [17]. In addition, Li has proposed dislocation ejection from stressed non-equilibrium grain boundaries as a mechanism that could explain grain growth in high purity nanograined metals deformed at low temperatures, based on an analysis of low angle tilt boundaries [22]. It has yet to be demonstrated that this theory can apply to general high angle boundaries and the lower purity (0.13% Mg) coarser grained samples of interest here.

The data below room temperature could of course also have been influenced by rapid static recovery on rewarming following PSC testing and due to the unavoidable delay in analysing the samples. However, the lack of significant coarsening in the samples held long term at room temperature suggests this is a small effect.

Overall, therefore, none of the above mechanisms satisfactorily explains the abnormally large boundary migration rates needed to maintain a constant grain size at cryogenic deformation temperatures, but do suggest a conventional thermally activated boundary migration model is inappropriate under these conditions. Although it is beyond the scope of this paper to propose a detailed mechanism, this would imply a collaborative process, or that there is breakdown in the law of proportionality between V and P (Eq. 4) at very high driving pressures and low temperatures.

Conclusions

The deformation structure evolution in a 0.1%Mg SMG alloy subjected to cryogenic deformation, and its subsequent stability during room temperature deformation, has been analysed by EBSD. Although a decreasing steady state minimum grain width was seen with reducing deformation temperature, a true nanocrystalline grain structure was not obtained, even at 77 K, and the HAB spacing only approached the nanoscale in one dimension. Deformation to an equivalent 98% rolling reduction at 77 K produced a microstructure comprising thin ribbon grains, with a minimum HAB spacing of 180 nm and a grain length still well over a micron. The cryogenically deformed material was found to be unstable on subsequent deformation at room temperature and underwent rapid dynamic grain growth.

It is shown that dynamic grain coarsening controls the limiting grain size obtainable in an SPD process. However, this occurs at an abnormally high rate compared to static grain growth. Either grain boundary diffusion, solute breakaway, or vacancy assisted HAB migration could potentially account for the enhanced rate of dynamic boundary migration observed under dynamic conditions at room temperature to moderate elevated temperatures, but are many orders of magnitude too slow at cryogenic temperatures. The abnormal boundary migration rates required to account for a steady state grain size at cryogenic temperatures are currently difficult to account for from existing theories of grain boundary migration.

Acknowledgements The authors would like to acknowledge F. J. Humphreys for helpful discussions and the financial support from the Manchester EPSRC Light Alloys, Portfolio Partnership (EP/D029201/1).

References

1. Prangnell PB, Huang Y, Berta M, Apps PJ (2007) Mater Sci Forum 550:159
2. Hebesberger T, Stüwe HP, Vorhauer A, Wetscher F, Pippan R (2005) Acta Mater 53:393. doi:10.1016/j.actamat.2004.09.043
3. Jazaeri H, Humphreys FJ (2004) Acta Mater 52:3239. doi:10.1016/j.actamat.2004.03.030
4. Jazaeri H, Humphreys FJ, Bate SP (2006) Mater Sci Forum 519–521:153
5. Duly D, Baxter GJ, Shercliff HR, Whiteman JA, Sellars CM, Ashby MF (1996) Acta Mater 44:2947. doi:10.1016/1359-6454(95)00392-4
6. Wang YM, Chen YM, Zhou F, Ma E (2002) Nature 419:912. doi:10.1038/nature01133
7. Wang YM, Ma E (2004) Acta Mater 521:1699. doi:10.1016/j.actamat.2003.12.022
8. Hayes RW, Rodriguez R, Lavernia EJ (2001) Acta Mater 49:4055. doi:10.1016/S1359-6454(01)00278-6
9. Jin M, Minor AM, Stach EA, Morris JW Jr (2004) Acta Mater 52:5381. doi:10.1016/j.actamat.2004.07.044
10. Gianola DS, Van Petegem S, Legros M, Brandstetter S, Van Swygenhoven H, Hemker KJ (2006) Acta Mater 54:2253. doi:10.1016/j.actamat.2006.01.023
11. Fan GJ, Fu LF, Choo H, Liaw PK, Browning ND (2006) Acta Mater 54:4781. doi:10.1016/j.actamat.2006.06.016
12. Brandstetter S, Zhang Kai, Escuadro A, Weertman JR, Van Swygenhoven H (2008) Scripta Mater 58:61. doi:10.1016/j.scriptamat.2007.08.042
13. Prangnell PB, Hayes JS, Bowen JR, Apps PJ, Bate PS (2004) Acta Mater 52:3193. doi:10.1016/j.actamat.2004.03.019
14. Hayes JS, Keyte R, Prangnell PB (2000) Mater Sci Tech 16:1259
15. Rauch EF (1992) Solid State Phenom 23–24:317
16. Balarin M (1975) Phys State Solid A 31:111. doi:10.1002/pssa.2210310259
17. Winning M, Gottstein G, Shvindlerman LS (2001) Acta Mater 49:211. doi:10.1016/S1359-6454(00)00321-9
18. Zehetbauer MJ, Steinter G, Schafler E, Korznikov A, Korznikova E (2006) Mater Sci Forum 503–504:57
19. Fu H-H, Benson DJ, Meyers MA (2001) Acta Mater 49:2567. doi:10.1016/S1359-6454(01)00062-3
20. Humphreys FJ, Hatherly M (2004) Recrystallization and related annealing phenomenon. Pergamon, Oxford, p 146
21. Suzuki A, Mishin Y (2005) Mater Sci Forum 502:157
22. Li JCM (2006) Phys Rev Lett 96:215506. doi:10.1103/PhysRevLett.96.215506